

Study on the accidental background of the JSNS² experiment

D. H. Lee^{a,1}, S. Ajimura², M. K. Cheoun³, J. H. Choi⁴, J. Y. Choi⁵,
T. Dodo^{6,9}, J. Goh⁷, K. Haga⁸, M. Harada⁸, S. Hasegawa^{9,8}, T. Hiraiwa²,
W. Hwang⁷, H. I. Jang⁵, J. S. Jang¹⁰, H. Jeon¹¹, S. Jeon¹¹, K. K. Joo¹²,
D. E. Jung¹¹, S. K. Kang¹³, Y. Kasugai⁸, T. Kawasaki¹⁴, E. J. Kim¹⁵,
J. Y. Kim¹², S. B. Kim¹⁶, W. Kim¹⁷, H. Kinoshita⁸, T. Konno¹⁴,
I. T. Lim¹², C. Little¹⁸, E. Marzec¹⁸, T. Maruyama¹, S. Masuda⁸,
S. Meigo⁸, S. Monjushiro¹, D. H. Moon¹², T. Nakano², M. Niiyama¹⁹,
K. Nishikawa¹, M. Y. Pac⁴, H. W. Park¹², J. S. Park^{b,17}, R. G. Park¹²,
S. J. M. Peeters²⁰, C. Rott^{21,11}, K. Sakai⁸, S. Sakamoto⁸, T. Shima²,
C. D. Shin¹, J. Spitz¹⁸, F. Suekane⁶, Y. Sugaya², K. Suzuya⁸, M. Taira¹,
Y. Yamaguchi⁸, M. Yeh²², I. S. Yeo⁴, C. Yoo⁷, I. Yu¹¹

¹High Energy Accelerator Research Organization (KEK), Tsukuba, Ibaraki, JAPAN

²Research Center for Nuclear Physics, Osaka University, Osaka, JAPAN

³Department of Physics, Soongsil University, Seoul 06978, KOREA

⁴Laboratory for High Energy Physics, Dongshin University, Chonnam 58245, KOREA

⁵Department of Fire Safety, Seoyeong University, Gwangju 61268, KOREA

⁶Research Center for Neutrino Science, Tohoku University, Sendai, Miyagi, JAPAN

⁷Department of Physics, Kyung Hee University, Seoul 02447, KOREA

⁸J-PARC Center, JAEA, Tokai, Ibaraki JAPAN

⁹Advanced Science Research Center, JAEA, Ibaraki JAPAN

¹⁰Gwangju Institute of Science and Technology, Gwangju, 61005, KOREA

¹¹Department of Physics, Sungkyunkwan University, Gyeong Gi-do, KOREA

¹²Department of Physics, Chonnam National University, Gwangju, 61186, KOREA

¹³School of Liberal Arts, Seoul National University of Science and Technology, Seoul, 139-743, KOREA

¹⁴Department of Physics, Kitasato University, Sagamihara 252-0373, Kanagawa, JAPAN

¹⁵Division of Science Education, Jeonbuk National University, Jeonju, 54896, KOREA

¹⁶School of Physics, Sun Yat-sen (Zhongshan) University, Guangzhou, 510275, China

¹⁷Department of Physics, Kyungpook National University, Daegu 41566, KOREA

¹⁸University of Michigan, Ann Arbor, MI, 48109, USA

¹⁹Department of Physics, Kyoto Sangyo University, Kyoto, JAPAN

²⁰Department of Physics and Astronomy, University of Sussex, Brighton, UK

²¹Department of Physics & Astronomy, The University of Utah, UT, 84112, USA

²²Brookhaven National Laboratory, Upton, NY, 11973-5000, USA

Received: date / Accepted: date

Abstract JSNS² (J-PARC Sterile Neutrino Search at J-PARC Spallation Neutron Source) is an experiment that searches for sterile neutrinos via the observation of $\bar{\nu}_\mu \rightarrow \bar{\nu}_e$ appearance oscillations using muon decay-at-rest neutrinos. The JSNS² experiment performed data taking from 2021. In this manuscript, a study of the accidental background is presented. The rate of the accidental background is $(9.29 \pm 0.39) \times 10^{-8}$ / spill with 0.75 MW beam power and comparable to the expected number of signal events.

1 Introduction

The existence of sterile neutrinos has been a crucial issue in the neutrino physics community for over 20 years. The experimental results from [1–6] could be interpreted as indications of the existence of sterile neutrinos with a mass-square differences of around 1 eV².

The JSNS² experiment, proposed in 2013 [7], is designed to search for neutrino oscillations due to a sterile neutrino at the Material and Life science experimental Facility (MLF) in J-PARC. MLF provides an intense and high-quality neutrino flux of 1.8×10^{14} ν /year/cm², from muon decay-at-rest (μ DAR) produced using a 1 MW proton beam with a 25 Hz repetition rate [8]. The neutrinos are produced by injecting 3 GeV protons from a

^ae-mail: leedh@post.kek.jp

^be-mail: jungsicpark@knu.ac.kr

rapid cycling synchrotron onto a mercury target in the MLF. The experiment uses a Gadolinium (Gd) loaded liquid scintillator (Gd-LS) detector with 0.1 w% Gd concentration placed at 24 m from the target.

The JSNS² experiment aims to perform a direct test of the LSND observation [1]. The same experimental principle used by the LSND experiment [1] to try and observe the $\bar{\nu}_\mu \rightarrow \bar{\nu}_e$ oscillation is used: inverse beta decay (IBD). There are several improvements offered by the JSNS² experiment. In order to identify IBD events, a delayed coincidence between the positron signal (prompt signal: up to 53 MeV) and neutron capture signal is used for selection. Gd is used to identify neutron captures. After capturing thermal neutrons on Gd, neutron capture on Gd generates gamma-rays with higher energies and shorter capture times (~ 8 MeV, ~ 30 μ s) than neutron capture on hydrogen (2.2 MeV, ~ 200 μ s). Therefore, accidental backgrounds coincident in the delayed signal region can be reduced by ~ 6 times compared to the hydrogen capture used in the LSND experiment, due to the shorter capture time. In addition, the short-pulsed beam, two 100 ns pulses in a 600 ns interval in each spill with a repetition of 25 Hz, enables us to set a timing window for the IBD prompt signal to 2.0 to 10 μ s from the proton beam collision so that the neutrinos from pion and kaon decay and fast neutrons generated at the target can be rejected efficiently. However, the efficiency for the μ DAR neutrinos can be kept at 48% because of the muon lifetime (2.2 μ s). The cosmogenic background is also reduced by a factor of 10^{-4} .

For JSNS², understanding the accidental background is essential since it is one of main backgrounds for the sterile neutrino search. Another important background, the correlated background, is described in [9]. A detailed discussion about the signal detection principle and the background rejection technique can be found in [7, 8].

2 Setup

The JSNS² experiment has been taking data with a single detector since 2021. Except for the beam maintenance period, which typically corresponds to a few months over the summer, the data has been accumulated continuously. The proton beam power has been increased from 600 kW in 2021 to 840 kW in 2023. There is usually a one-day facility maintenance per week and we continue to take data during that time to acquire beam-off data. The integrated number of proton-on-target (POT) collected was 2.94×10^{22} , corresponding to less than $\sim 28.0\%$ of the required POT of the JSNS² experiment.

To understand the rate and properties of the accidental background, dedicated calibration data were taken. The accelerator-driven timing signal was used for the trigger [10, 11], which caused a 125 μ s time window for data acquisition system (FADC) to be opened, with no energy bias. The total available number of spills is 2.46×10^6 , therefore the expected number of IBD signal events from this calibration run is estimated to be much less than 1 [8]. Thus, all observed events are likely to be background.

2.1 Experimental setup

The JSNS² detector is a cylindrical liquid scintillator detector with 4.6 m diameter and 3.5 m height located at a distance of 24 m from the mercury target of the MLF. It consists of 17 tonnes of Gd-LS contained in an acrylic vessel, and 33 tonnes unloaded liquid scintillator (LS) in a layer between the acrylic vessel and a stainless steel tank. The LS and the Gd-LS consist of LAB (linear alkyl benzene) as the base solvent, 3 g/L PPO (2,5-diphenyloxazole) as the fluor, and 15 mg/L bis-MSB (1,4-bis(2-methylstyryl) benzene) as the wavelength shifter. The LS volume is separated into two independent volumes by an optical separator. The region inside the optical separator, called the “inner detector”, consists of the entire volume of the Gd-LS and ~ 25 cm thick LS layer. Scintillation light from the inner detector is observed by 96 Hamamatsu R7081 photomultiplier tubes (PMTs) each with a 10-inch diameter. The outer layer, called the “veto layer”, is used to detect cosmic-ray induced particles coming into the detector. A total of 24 of 10-inch PMTs are set in the veto layer. On the whole inner surfaces of the veto layer, reflection sheets are attached in order to improve the collection efficiency of the scintillation light.

2.2 Data acquisition and trigger system

PMT signal waveforms from both the inner detector and the veto layer are digitized and recorded at a 500 MHz sampling rate by 8-bit flash analog-to-digital converters (FADCs). As a trigger, we utilize a 25 Hz periodic signal from the accelerator scheduled timing which directs the proton beam towards the MLF target, called the “kicker trigger”. The width of the acquired waveform in this trigger scheme is set to 125 μ s, which fully covers the prompt and delayed signal timing window of the IBD events. The rate limitation of the JSNS² data acquisition system under this condition is 5 Hz, thus, a pre-scaling factor of 5 is required. We mainly used this trigger and data acquisition to obtain the beam-on

data for an accidental background estimation within the sterile neutrino search.

Detailed description of the detector and the triggers are given in [10, 11], respectively.

3 Event selection

The data set used for the background estimation was obtained using the kicker trigger. The total number of beam spills was 2460399, equivalent to ~ 6 days of data taking with a pre-scale factor of five. Given the readout 125 μs time, the obtained waveforms contain multiple events. We therefore used an event definition based on the number of hit PMTs in order to extract each event. We constructed a hit time and charge series at each trigger by accumulating hit information along the FADC window with 60 ns coincidence width over all the PMTs. The coincidence width was determined by considering a typical PMT pulse shape and a safety factor from timing calibration. The event discrimination threshold is set to 10 hits and 50 p.e., which corresponds to an energy well below 1 MeV.

The event vertex position and energy reconstruction is performed simultaneously based on a maximum-likelihood algorithm using the charge response of each PMT. Both vertex position and energy were calibrated by deploying a ^{252}Cf source and using the 8 MeV peak in the energy spectrum resulting from thermal neutron capture on Gd (nGd). The reconstruction performance can be found in [12] for nGd events and in [13] for events with up to 60 MeV using Michel electrons.

The selection criteria and estimated efficiency are given in Table 1 and a more detailed description is found in [8]. Each efficiency in Table 1 is for each corresponding criterion only.

The single rates of the prompt and the delayed candidates are separately estimated using the energy and the timing selections shown in Table 1. Note that a time difference from the beam collision timing, $5 \leq \Delta t_{\text{beam-d}} \leq 105 \mu\text{s}$ is used for the delayed single rate calculation instead of the selection in Table 1. These single rates are multiplied to predict the number of the accidental backgrounds. The fiducial volume is defined with $R < 140 \text{ cm}$ and $|z| < 100 \text{ cm}$ region to avoid external backgrounds. Note that origin of the coordinate system is the center of the detector, and R is defined as $R = \sqrt{x^2 + y^2}$.

The prompt IBD candidates are selected using a time difference from beam collision timing ($\Delta t_{\text{beam-p}}$) and its energy (E_p). We applied the following requirements; $2 \leq \Delta t_{\text{beam-p}} \leq 10 \mu\text{s}$ and $20 \leq E_p \leq 60 \text{ MeV}$, in order to fully cover μDAR neutrinos from the mercury target. The timing selection rejects beam-induced

Table 1 The IBD selection criteria and their efficiencies in the JSNS² experiment [8]. The single rates of the prompt and the delayed candidates are estimated separately using the energy and the timing selection in this table. Note that the timing window: $5 \leq \Delta t_{\text{beam-d}} \leq 105 \mu\text{s}$ is used for the delayed single rate calculation. Each efficiency is for to each corresponding criterion only.

Requirement	Efficiency /%
–Prompt Event–	
$20 \leq E_p \leq 60 \text{ MeV}$	92
$2.0 \leq \Delta t_{\text{beam-p}} \leq 10 \mu\text{s}$	48
Pulse Shape Discrimination	99
–Delayed Event–	
$7 \leq E_d \leq 12 \text{ MeV}$	71
$\Delta\text{VTX}_{\text{OB-d}} \geq 110 \text{ cm}$	98
–IBD paired Event–	
$\Delta t_{\text{p-d}} \leq 100 \mu\text{s}$	93
$\Delta\text{VTX}_{\text{p-d}} \leq 60 \text{ cm}$	96
Timing likelihood	91
Total	25

fast neutrons in the beam on-bunch timing ($0 \leq \Delta t_{\text{beam-p}} \leq 1.5 \mu\text{s}$) as well as neutrino backgrounds from kaon and pion decay whose lifetimes are 12 ns and 26 ns, respectively.

In order to identify neutron captures on Gd, the 8 MeV peak of the delayed signal energy (E_d) is selected using a requirement of $7 \leq E_d \leq 12 \text{ MeV}$ [14]. There are nGd events associated with fast neutrons induced by the beam contributing to the IBD delayed candidates as an accidental background [15]. Pulse Shape Discrimination (PSD) is used within the IBD prompt timing region to reduce neutrons induced by cosmic rays as shown in [9]. However, it is optimized for the energy range of $20 \leq E_p \leq 60 \text{ MeV}$. Thus, we need another strategy to reject those nGd events. Since these nGd events correlate spatially with an activity made by beam-induced fast neutrons, we can reject them with the spatial correlation. In particular, we applied a requirement on the spatial difference between on-bunch events and delayed candidates, $\Delta\text{VTX}_{\text{OB-d}} \geq 110 \text{ cm}$. The distribution of $\Delta\text{VTX}_{\text{OB-d}}$ and the efficiency estimation can be found in [14]. The on-bunch event tagging condition is set to $0 \leq \Delta t_{\text{beam-OB}} < 1.5 \mu\text{s}$ and $1 \leq E_{\text{OB}} \leq 200 \text{ MeV}$.

Figure 1 demonstrates the energy and timing selection windows in a two-dimensional distribution of energy and timing. The red and green boxes represent the prompt and delayed signal regions. The beam on-bunch event are also defined as an orange dashed box.

The events induced from muons or incoming particles from outside are rejected from both prompt and delayed candidates by the veto region of the detector. The events which have more than 30 photo-electrons

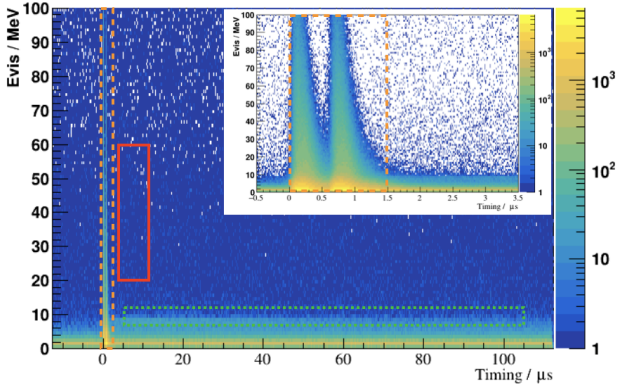


Fig. 1 A two-dimensional distribution of energy and timing before event selection, used to demonstrate the IBD selection region. The selected regions for the IBD prompt candidate from positron (red solid box), the IBD delayed candidate from gamma-rays resulted in thermal neutron capture on Gd (green dashed box) and the beam on-bunch event (orange dashed box) are overlaid. Note that the events are shown around the prompt signal timing region. There are two event clusters within 0 to 1.5 μs , which reflect the proton beam structure of the MLF. They are caused by neutrons produced at the mercury target. One can see that the IBD prompt signal region is well separated from the on-bunch region. The events in the IBD delayed signal region must also satisfy $\Delta t_{p-d} > 0$ in the actual delayed coincidence.

(p.e.) of a total charge for the top-side 12 PMTs or 40 p.e. for the bottom-side 12 PMTs are rejected.

The decayed Michel electrons (ME) from muon decay are also crucial background. The IBD candidates are rejected if parent muons are found during 10 μs before the candidate. The events that have more than 100 p.e. for the top 12 or bottom 12 PMTs are categorized as parent muons except for the beam timing. At the beam timing, incoming neutrons induced by the beam (0.7464 ± 0.0006 / spill) could pass the criteria for selecting parent muons; thus we applied a different condition only during the beam timing. The equation $E + Q_{veto}/9 > 200$ is used to define the parent muons of Michel electrons during the beam timing, where E is the deposited energy in the target and catcher regions and Q_{veto} is the total charge of veto region with p.e. unit. “ $Q_{veto}/9$ ” converts p.e. to MeV units in the equation. For example, $Q_{veto} = 9$ p.e. corresponds to 1 MeV in the veto region.

Fig. 2 shows the distributions of E_p (a), E_d (b) and T_p from beam (c), T_d from beam (d) after applying the IBD selection.

The number of selected events of the IBD prompt and the delayed candidates are 542 and 44336, respectively, thus the single rates for those are $(2.20 \pm 0.09) \times 10^{-4}$ / spill (prompt) and $(1.80 \pm 0.01) \times 10^{-2}$ / spill (delayed), respectively. Note that the uncertainties men-

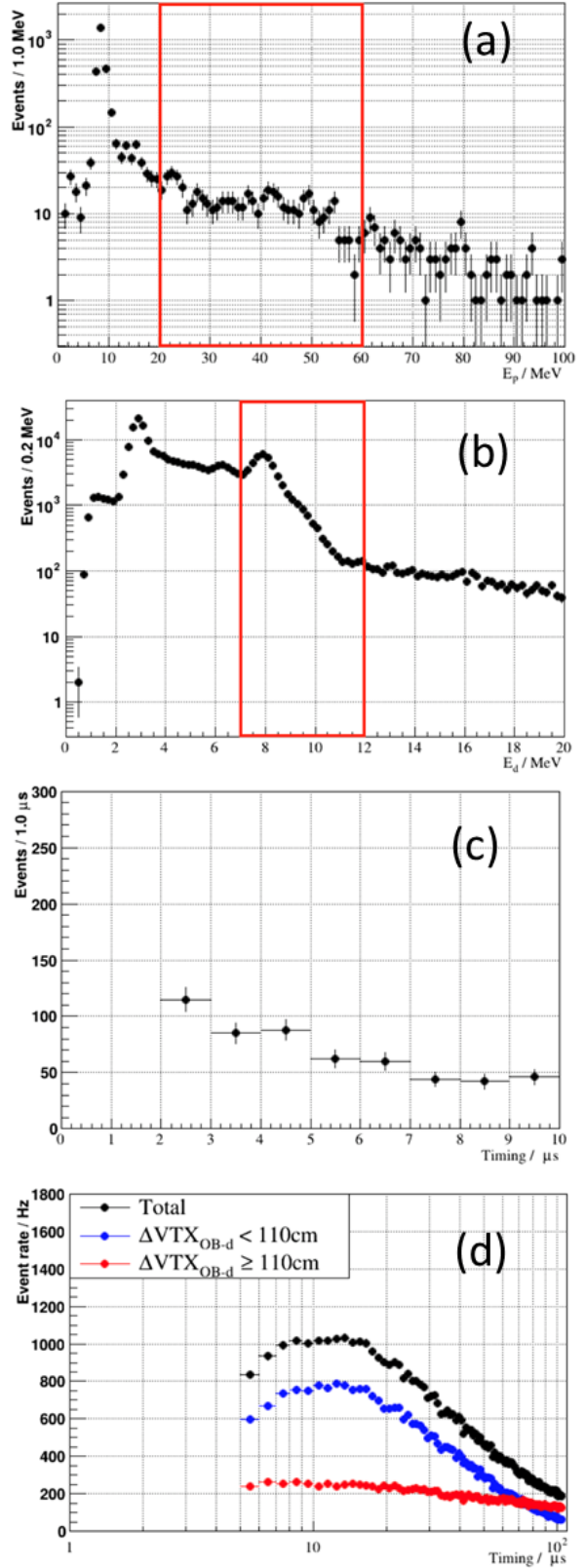


Fig. 2 The distributions of the variables used in the IBD selection: (a) E_p , (b) E_d , (c) T_p from beam timing and (d) T_d from beam. Each distribution has all of the selection criteria applied, except for the selection on the variable displayed. The red boxes show the selection criteria for E_p and E_d .

Table 2 The beam power dependence of the rate of the IBD prompt and delayed candidates.

Beam power	prompt Rate / spill	Delayed rate / spill
0 (beam off)	$(1.85 \pm 0.20) \times 10^{-4}$	$(3.98 \pm 0.09) \times 10^{-3}$
750 kW	$(2.20 \pm 0.09) \times 10^{-4}$	$(1.80 \pm 0.01) \times 10^{-2}$

tioned in this paper contain both the statistical and systematic uncertainties. For the systematic uncertainties, the energy scale, the FADC timing and the reproducibility are considered. Figure 2 (d) shows that the rejection using spatial correlation between beam neutrons and delayed candidates (ΔVTX_{OB-d}) works well.

4 Beam on-off comparison of single rates

The comparison of single rates between beam-on and beam-off are also performed. The beam-off data is also taken using the the kicker trigger with 125 μs , and the IBD event selection is identical to that in beam-on data. The total number of the beam-off triggers is 466,348, which is equivalent to about 1 day of data taking. Table 2 shows the comparison of the IBD prompt and delayed candidates.

This result shows the rate of the IBD prompt background are independent from the beam power, which indicates that the cosmic ray induced particles are dominated in this region. On the other hand, that of the delayed background has large dependence of the beam.

5 Accidental background rates

The accidental background rate is evaluated by multiplying the single rates as follows:

$$R_{acc.} \sim R_p \times R_d \times \epsilon_{cut} \quad (1)$$

where R_{acc} is the accidental background rate (/spill), R_p is the single rate of the IBD prompt candidates (/spill), and R_d is the rate of of delayed candidates (/spill). If the additional selections are applied, the selection efficiency to the accidental background (ϵ_{cut}) should be also multiplied. As shown in Table 1, the spatial correlation selection between the prompt and delayed candidates, ΔVTX_{p-d} , and timing likelihood should also be considered. In this manuscript, only the spatial correlation cut is described. The likelihood will be considered in a different future paper.

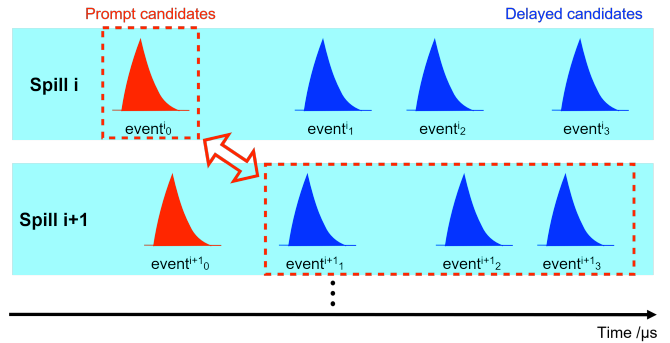


Fig. 3 The principle of the spill shift.

Table 3 The numbers used in Equation 1 and the calculated accidental background.

	Value
Prompt Rate / spill	$(2.20 \pm 0.09) \times 10^{-4}$
Delayed Rate / spill	$(1.80 \pm 0.01) \times 10^{-2}$
Efficiency of $\Delta VTX_{p-d} \leq 60$ cm	$5.1 \pm 0.1\%$
Efficiency of Timing likelihood [8]	46%
Accidental Rate / spill / 0.75MW	$(9.29 \pm 0.42) \times 10^{-8}$

5.1 Evaluation of the spatial cut efficiency using a spill shift method

In order to evaluate the efficiency of ΔVTX_{p-d} of the pure accidental uncorrelated background, a novel technique is invented, which we call “spill shift method”. Within the same beam spill, the correlated background is dominating, as discussed in [9]. However, if we use subsequent spills, beam correlated events disappear after more than 40 ms and thus a pure sample of uncorrelated accidental events is obtained. Once the IBD prompt candidate in one spill is found, the different beam spills are analyzed to find the paired delayed candidates. At first, the next beam spill of the spill that have the IBD prompt candidate is used. Secondly, the beam spill that is different by two spills from the spill with IBD prompt candidate is used. This process is repeated from the 1st to the 10,000th next spills to get higher statistics. Figure 3 shows the cartoon illustrating the principle of the spill shift in the case of 1 spill shift.

Figure 4 shows the estimated ΔVTX_{p-d} distribution. The estimated efficiency of the $\Delta VTX_{p-d} \leq 60$ cm cut is $5.1 \pm 0.1\%$.

5.2 Accidental background rates

The expected accidental background rate is $(9.29 \pm 0.42) \times 10^{-8}$ / spill / 0.75MW using the Equation 1. The numbers used in this calculation of the accidental back-

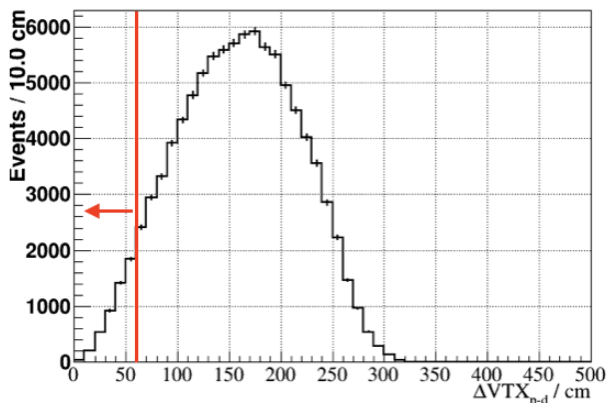


Fig. 4 The estimated ΔVTX_{p-d} distribution of the accidental background with the spill shift method. The red line shows a cut value, and the remained fraction of the accidental background is $5.1 \pm 0.1\%$.

ground rate are summarized in Table 3. The single rates, the spatial correlation cut efficiency mentioned above and the assumed efficiency of timing likelihood ($\sim 46\%$) described in [8] are used.

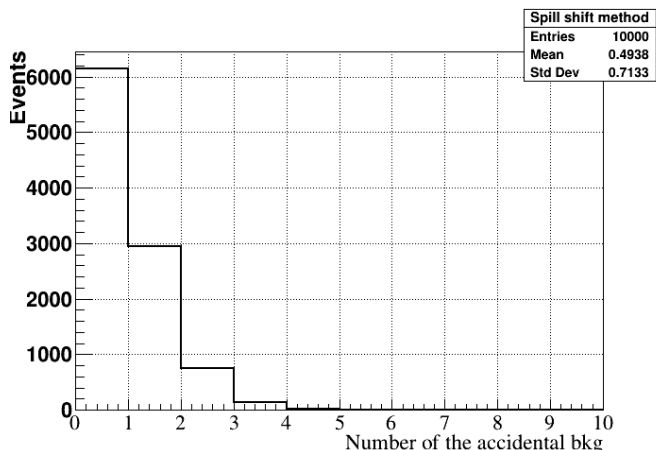


Fig. 5 The expected number of accidental background events from the spill shift method during this calibration run with 2,460,399 spills after the $\Delta VTX_{p-d} \leq 60$ cm cut. This is for the complementary method to estimate the accidental background rate.

The spill shift method can also be utilized to estimate the rate of the accidental backgrounds independently from the single rates method because each n -th spill shift case can find number of accidental background events in this control sample, individually. Figure 5 shows the number of accidentally paired background events in each spill shift cases (1,2, ... 10,000 spills shift) during 2,460,399 spills after the ΔVTX_{p-d} cut, i.e.; one certain n -th spill shift case provides one entry in this histogram. The mean of the Poisson dis-

tribution is 0.494 ± 0.008 events over 2,460,399 spills, thus the estimated accidental background rate is $(9.24 \pm 0.15) \times 10^{-8}$ / spill / 0.75MW. This is consistent with the single rates method.

The expected oscillation IBD signal rate is 4.59×10^{-8} / spill / MW [8] with the LSND best fit oscillation parameters. Thus, JSNS² has a comparable accidental background rate as the expected neutrino oscillation signal with the LSND best fit oscillation parameters.

6 Summary

JSNS² aims to perform a direct test of the positive result of the LSND experiment using a decay-at-rest neutrino source at the MLF and a Gd-LS detector. We started data taking in 2021.

The calibration runs with the accelerator scheduled timing to study the accidental background have been performed. As a result, the single rates of the IBD prompt and delayed candidates at 0.75 MW of averaged beam power are $(2.20 \pm 0.09) \times 10^{-4}$ / spill and $(1.80 \pm 0.01) \times 10^{-2}$ / spill, respectively. The expected rate of the accidental background is $(9.29 \pm 0.39) \times 10^{-8}$ / spill, which is a similar level with that of the IBD neutrino oscillation signal with the LSND best fit oscillation parameters. We anticipate the future improvements to reduce the accidental background with sophisticated likelihood and/or machine-learning techniques.

Acknowledgements We thank the J-PARC staff for their support. We acknowledge the support of the Ministry of Education, Culture, Sports, Science, and Technology (MEXT) and the JSPS grants-in-aid: 16H06344, 16H03967 and 20H05624, Japan. This work is also supported by the National Research Foundation of Korea (NRF): 2016R1A5A1004684, 2017K1A3A7A09015973, 2017K1A3A7A09016426, 2019R1A2C3004955, 2016R1D1A3B02010606, 2017R1A2B4011200, 2018R1D1A1B07050425, 2020K1A3A7A09080133, 2020K1A3A7A09080114, 2020R1I1A3066835, 2021R1A2C1013661 and 2022R1A5A1030700. Our work has also been supported by a fund from the BK21 of the NRF. The University of Michigan gratefully acknowledges the support of the Heising-Simons Foundation. This work conducted at Brookhaven National Laboratory was supported by the U.S. Department of Energy under Contract DE-AC02-98CH10886. The work of the University of Sussex is supported by the Royal Society grant no. IESnR3n170385. We also thank the Daya Bay Collaboration for providing the Gd-LS, the RENO collaboration for providing the LS and PMTs, CIEMAT for providing the splitters, Drexel University for providing the FEE circuits and Tokyo Inst. Tech for providing FADC boards.

References

1. C. Athanassopoulos et al. (LSND Collaboration), Phys. Rev. Lett. **77** (1996) 3082.
2. W. Hampel et al. (GALLEX Collaboration), Phys. Lett. B **420** (1998) 114.
3. J. N. Abdurashitov et al. (SAGE Collaboration), Phys. Rev. C **80** (2009) 015807.
4. G. Mention, M. Fechner, T. Lasserre, T. A. Mueller, D. Lhuillier, M. Cribier and A. Letourneau, Phys. Rev. D **83** (2011) 073006.
5. A. A. Aguilar-Arevalo et al. (MiniBooNE Collaboration), Phys. Rev. Lett. **110** (2013) 161801.
6. A. A. Aguilar-Arevalo et al. (MiniBooNE Collaboration), Phys. Rev. Lett. **120** (2018) 141802.
7. M. Harada, et al, arXiv:1310.1437 [physics.ins-det]
8. S. Ajimura, et al, arXiv:1705.08629 [physics.ins-det]
9. Y. Hino et al. (JSNS² Collaboration), Eur. Phys. Journal C **82** (2022) 331
10. S. Ajimura et al, Nucl. Inst. Meth. A 1014 (2021) 165742
11. J. S. Park, et al, 2020 JINST **15** T09002
12. J. R. Jordan's PhD thesis,
<https://dx.doi.org/10.7302/6288>
13. H. K. Jeon's PhD thesis,
https://www.riss.kr/search/detail/DetailView.do?p_mat_type=be54d9b8bc7cdb09&control_no=23512b6c011ad455ffe0bdc3ef48d419
14. M. Harada, et al, arXiv:1502.02255 [physics.ins-det]
15. S. Ajimura et al, PTEP 2015 6, 063C01 (2015).